Available online at www.sciencedirect.com
SCIENCE DIRECT®
Journal of Molecular Catalysis A: Chemical 216 (2004) 199–207
JOURNAL OF MOLECULAR CATALYSIS A: CHEMICAL
www.elsevier.com/locate/molcata

In situ characterization of the adsorption of cinchona chiral modifiers on platinum surfaces☆

Zhen Ma, Ilkeun Lee, Jun Kubota[1], Francisco Zaera*

Department of Chemistry, University of California, Riverside, CA 92521, USA

Abstract

The adsorption of cinchona chiral modifiers on platinum surfaces has been characterized with surface-sensitive techniques. The uptakes of quinoline and lepidine, models for the aromatic moiety of the cinchona, were first studied on Pt(1 1 1) single crystal surfaces and under ultrahigh vacuum by reflection–absorption infrared spectroscopy (RAIRS). Adsorption at low (∼100 K) temperatures is molecular and without any preference for a distinct molecular geometry. Temperature programmed desorption (TPD) experiments indicated extensive dehydrogenation starting at about 250 K, and infrared data obtained at room temperature corroborated the conversion of some of the aromatic C–H bonds to a more aliphatic environment. An in situ RAIRS characterization of the adsorption of cinchonidine from carbon tetrachloride solutions onto a polycrystalline platinum substrate proved that in hydrogen-treated solvents the decomposition of the adsorbate is inhibited, so that the cinchona retains its molecular character on the surface at room temperature. Three adsorption regimes were identified depending on the concentration of cinchonidine in solution, namely, no observable adsorption at low concentrations, bonding via a flat-lying quinoline moiety in the intermediate concentration range, and a tilted adsorption geometry near saturation. The optimum activity and enantioselectivity reported previously in catalytic processes for intermediate concentrations can then be associated with the orientation of the aromatic ring parallel to the surface plane. In a separate study, it was determined that hydrogen plays a unique role in cinchonidine adsorption, initially conditioning the surface for the uptake (presumably by reduction and removal of surface contaminants), and later hydrogenating the quinoline fragment of the modifier and facilitating its desorption. Finally, different solvents were shown to behave differently in these systems. Specifically, adsorbed cinchonidine remains on the platinum surface after flushing with non-polar solutions such as cyclohexane, but can be easily removed by more polar solvents such as dichloromethane. This behavior correlates well with both the solubility of cinchonidine and the performance of the cinchona/platinum catalyst as a function of the nature of the solvent.

Keywords: Cinchonidine; Platinum; Enantioselective hydrogenation; Catalysis; Solid–liquid interface; In situ reflection–absorption infrared spectroscopy

1. Introduction

Molecular chirality in organic molecules, the consequence of a non-symmetrical arrangement of different ligands around a given carbon atom, is critical in biochemistry, because nature has evolved to favor one of the two possible (R or S) enantiomers over the other [1,2]. Production of racemic (R:S = 50:50) mixtures for biological applications is at best a waste of material, and can even be deadly, as in the case of the drug thalidomide, which was first marketed in the 50's in racemic form as a mild analgesic without realizing that one of the enantiomers causes fetal malformations [3]. The problem is that since most of the physical properties of the two enantiomers of a given compound are identical, their separation is difficult. The preference for processes which produce enantiomerically pure chemicals instead is manifested by their growing share of the pharmaceutical and chemical industries: the market for single enantiomers has recently reached the US $ 160 billion mark in sales, and already accounts for close to half of the profits from sales of drugs worldwide [4].

A number of approaches are already available for the manufacturing of enantiomerically pure compounds. For instance, racemic mixtures can be separated by techniques such as chiral chromatography or by reactions with other chiral compounds [5,6]. This is quite wasteful, however, so

☆ For the special issue 'Heterogeneous Chiral Catalysis'.

* Corresponding author. Tel.: +1-909-7875498; fax: +1-909-7873962.
E-mail address: francisco.zaera@ucr.edu (F. Zaera).
[1] Present address: Chemical Resources Laboratory, Tokyo Institute of Technology, 4259 Nagatsuda Midoriku, Yokohama 226-8503, Japan.

1381-1169/$ – see front matter © 2004 Elsevier B.V. All rights reserved.
doi:10.1016/j.molcata.2004.03.012

the direct production of single enantiomers by bio, homogeneous, or heterogeneous catalysis is much more desirable. Asymmetric synthesis with biocatalysts is common in applications such as the reduction of carbonyl compounds with bakers' yeast for the production of optically active alcohols [7], and cleaner processes employing isolated enzymes are also available [8,9]. Nevertheless, the purification of enzymes is laborious, and their reactions are often slow and limited in terms of substrate specificity [10,11]. At present, homogeneous catalysis, in particular that based on the use of metal complexes with chiral ligands, provides the most versatile approach to enantioselective chemical synthesis [12–14]. Unfortunately, metal complexes are expensive, hard to handle, and difficult to separate from the products. In addition, homogeneous catalysis often requires high pressures, and that makes the processes dangerous and adds to its cost. It is therefore highly desirable to develop alternative heterogeneous enantioselective catalysts.

In spite of its desirability, heterogeneous catalysis has so far had little impact in the manufacturing of enantiomerically pure compounds. One promising direction in this area is the use of chiral modifiers, in particular for the hydrogenation of C=O double bonds. The initial report on the hydrogenation of β-ketoesters over nickel catalysts modified with tartaric acid provided a good example of the viability of this approach [15–18]. Since then, there have also been a number of studies on the hydrogenation of α-ketoesters on supported platinum catalysts modified with cinchona alkaloids [19–22]. Both platinum and palladium have been used for a few other enantioselective catalytic reactions in recent years [23,24], but the scope of chiral modification in heterogeneous catalysis remains limited. This is in great part due to the present lack of understanding of the basic mechanism behind these processes.

In the cinchona/platinum system, the chiral modifier is proposed to consist of three main components, namely, a quinoline aromatic ring for adsorption, a quinuclidine tertiary amine to complex with the reactant, and a stereogenic region around the C8-C9 carbons to facilitate the preferential hydrogenation of one of the faces of the carbonyl group of the reactant (Fig. 1) [20,25]. Numerous studies have examined the role of the modifier structure and substituting groups [25–27], the modifier concentration [19,28], the interaction between modifier and reactant [29–32], the nature of the solvent [33–35], the particle size and catalyst support [36–39], and the reaction conditions [40–42] on the activity and selectivity of these processes. By optimizing these variables, enantiomeric excesses as high as 95% have been reached in selected cases [22,28]. At the same time, those studies have highlighted the complexity of such chiral modification. It appears that to be able to design chiral catalytic systems for the manufacturing of specific chemicals it is necessary to develop a better microscopic picture of the chemical phenomena involved at the liquid–solid interface. In our laboratory we have embarked on the in situ characterization of the adsorption and catalytic chemistry of cinchona chiral modifier on platinum catalytic surfaces. Our results so far, together with those of other groups [43–45], point to the general conclusion that the catalytic performance of the cinchona/platinum system depends directly on the adsorption characteristics of the chiral modifier. In the following paragraphs the observations derived from our work on the effect of concentration, hydrogen pretreatment, and nature of the solvent on cinchona chiral modifiers are briefly reviewed.

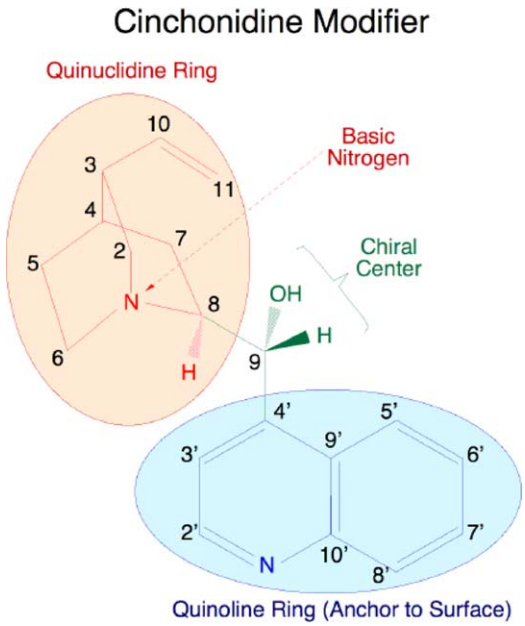

Fig. 1. Schematic representation of the molecular structure of cinchonidine, highlighting the three main fragments relevant to its chiral modification properties, namely, a quinoline aromatic ring responsible for adsorption to the platinum surface, a quinuclidine tertiary amine believed to form a 1:1 complex with the carbonyl group of the α-ketoester reactant, and a chiral center that facilitates the particular orientation of the reactant needed for its enantioselective hydrogenation [20,25]. Numbers are assigned to each carbon atom to facilitate the discussion on adsorption geometry.

2. Experimental

Initial experiments on the adsorption of quinoline and lepidine were carried out under ultrahigh vacuum (UHV) conditions by using equipment and procedures discussed in detail in previous studies of other systems [46–48]. The stainless steel chamber used for this is cryopumped to a base pressure below 1×10^{-10} Torr, and is equipped with an ion gun for sputtering of the surface, an UTI-100C quadrupole mass spectrometer for temperature-programmed desorption (TPD), and a Bruker Equinox 55 Fourier-transform infrared (FTIR) spectrometer for reflection–absorption infrared spectroscopy (RAIRS). The quadrupole mass spectrometer was retrofitted with an extendable nose cone with a 5-mm diameter aperture which can be placed within 1 mm of the front face of the single crystal for the selective detection of desorbing molecules during the TPD experiments. The quadrupole

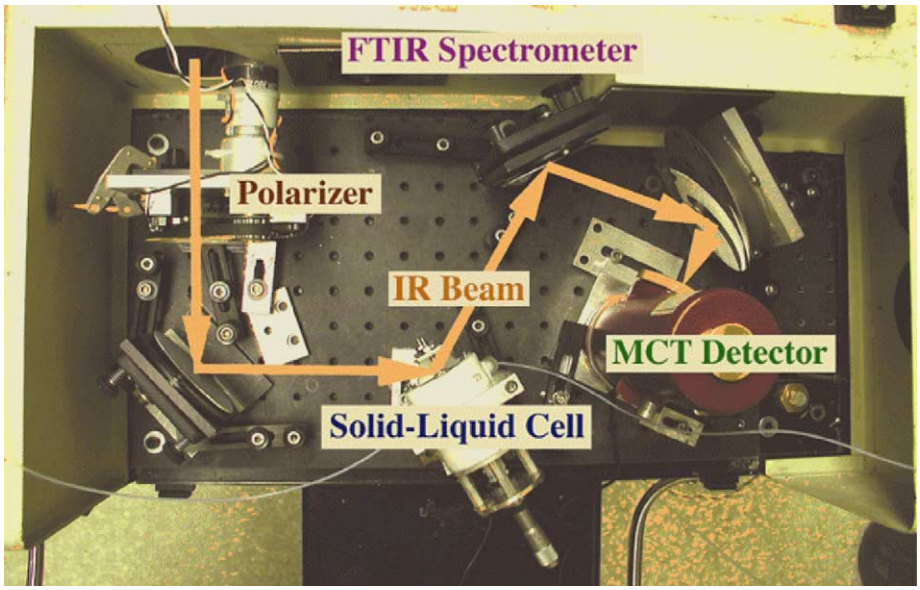

Fig. 2. Top view of the experimental setup used for the in situ reflection–absorption infrared spectra characterization of the adsorption of cinchonidine from solutions onto Pt surfaces [50]. The infrared beam from the Fourier-transform infrared spectrometer is directed and focused onto a polished platinum surface placed in a solid–liquid cell. This cell consists of the platinum disk used as the surface for our adsorption studies, a CaF_2 prism for optical guidance of the infrared beam, and a liquid solution trapped between those two elements. The reflected beam is then collected by a mercury-cadmium-telluride (MCT) detector. The overall arrangement also includes gas and liquid sample introduction stages, and a set of electronics for electrochemical oxidation–reduction cleaning of the Pt surfaces.

spectrometer is interfaced with a personal computer capable of monitoring the time evolution of up to 15 different masses in a single experiment, and heating rates of 10 K/s are set by a homemade temperature controller. The RAIRS experiments were performed by focusing the infrared beam from the FTIR spectrometer through a sodium chloride window onto the sample in the UHV chamber and by collecting the reflected beam, after passing through a second sodium chloride window and a polarizer, onto a mercury-cadmium-telluride (MCT) detector. Grazing incidence was used to optimize the signal from the surface species. Either 1000 or 2000 scans, taken with $4\,cm^{-1}$ resolution, were averaged and ratioed against spectra from the clean surface recorded immediately before dosing. The RAIRS data were taken at sample temperatures around 100 K unless otherwise indicated. The platinum single crystal was cut in the (1 1 1) orientation and polished to a mirror finish using standard procedures, and mounted via two bridging tantalum wires to a sample holder which can be cooled with liquid nitrogen and heated resistively to any temperature between 90 and 1200 K, as monitored by a chromel–alumel thermocouple spot-welded to the edge of the crystal. The sample was cleaned between experiments by heating at 700 K in 3×10^{-7} Torr of O_2 for several minutes to remove any residual carbon, and was periodically monitored for contamination by examining the quality of oxygen TPD [49].

RAIRS experiments were also performed in situ to characterize the liquid–solid interface during adsorption of cinchona modifiers from solution onto a polished platinum disk. The experimental setup, a picture of which is provided in Fig. 2, has been described in detail previously [50,51]. Briefly, the RAIRS measurements were performed by using a solid–liquid cell in which a thin liquid film of the solution of interest is trapped in between the surfaces of the prism and the metal. The platinum disk is held by a micrometer to allow for its retraction before and after each measurement in order to refresh the liquid solution. The inlet and outlet tubes used to feed the solutions are connected to a gas handling system in order to be able to bubble and saturate the solution with specific gases as needed. The solid sample is cleaned by oxidation–reduction electrochemical cycles, and deemed clean when the RAIRS data for carbon monoxide adsorption reported in the literature is reproduced. The IR beam from a Mattson Sirius 100 FTIR spectrometer is focused through a polarizer and the CaF_2 prism onto the Pt surface, and refocused onto a liquid N_2-cooled mercury-cadmium-telluride (MCT) detector. A grazing incidence angle of 60° into the prism was chosen to avoid total internal reflection at the prism–solution interface. Ratios of p/s polarization spectra were used to discriminate between adsorbed and dissolved species.

3. Vacuum adsorption

Initial experiments were carried out under controlled vacuum conditions in order to characterize the adsorption of the quinoline ring in cinchona on Pt(1 1 1) single crystal surfaces. RAIRS spectra for quinoline and lepidine (4-methyl quinoline), simplified models for the aromatic moiety of the

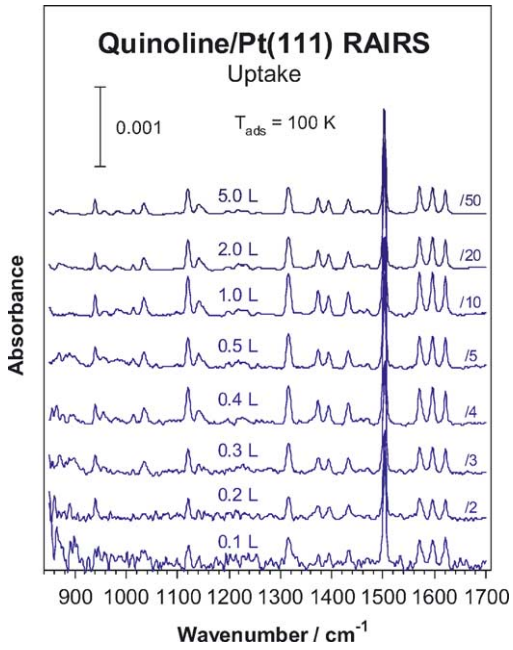

Fig. 3. RAIRS data for quinoline adsorbed on a Pt(1 1 1) single crystal surface at 100 K as a function of initial exposure. These experiments were carried out under ultrahigh vacuum conditions. The shapes and positions of most infrared absorption peaks are quite similar at all coverages, while the intensities grow linearly with exposure. This suggests a molecular adsorption without any preferential surface geometry. A detailed assignment of the vibrational modes is provided in Table 1.

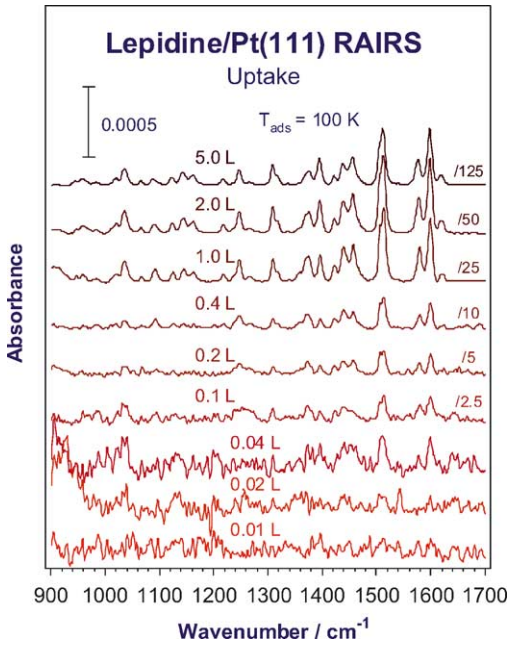

Fig. 4. Similar RAIRS uptake sequence for lepidine (4-methyl quinoline) on Pt(1 1 1). This is a better model for the aromatic moiety of cinchonidine, because it includes a carbon–carbon bond at the position where the chiral center and the quinuclidine fragment attach to the quinoline moiety in the cinchona. Again, the general features of the spectra are similar at all coverages, indicating molecular and non-preferential adsorption. A detailed assignment of the vibrational modes is provided in Table 1.

cinchona modifier [52], are reported in Figs. 3 and 4, respectively, as a function of exposure at 100 K. In both cases molecular adsorption was seen at all coverages, as indicated by the similarities of the data with spectra obtained for condensed multilayers of the same compounds (monolayer saturation was estimated by TPD to be reached roughly about 1–3 L, data not shown). The vibrational assignment can be easily made by using previous theoretical [53,54] and experimental [55–57] reports for the pure compounds as well as other related references [58], and is provided in Table 1. Note that most of the deformation modes seen in the 800–1700 cm^{-1} region displayed in Figs. 3 and 4 correspond to in-plane molecular motions, mainly associated with the entire ring. Based on the so-called surface selection rule that applies to RAIRS of adsorbates on metals, the infrared absorption cross sections for in-plane and out-of-plane vibrational modes respond differently to changes in adsorption geometry [59–61]. The lack of any obvious variations in relative intensities among the various vibrational modes between the pure liquids and the adsorbed species suggests that there is no preferred adsorption geometry at these low temperatures.

Adsorption of either quinoline or lepidine at room temperature under vacuum leads to extensive decomposition. No clear infrared spectra could be obtained for the resulting surface species because of their weak signals. Nevertheless, loss of aromaticity could be determined by the changes in the C–H stretching region of the RAIRS spectra and by the shifts from the aromatic peaks about 3005, 3038, and 3055 cm^{-1} for pure quinoline (and about 3006, 3035, and 3060 cm^{-1} for lepidine) to a set of new features between 2900 and 2970 cm^{-1} (data not shown). This conclusion is supported by the TPD data in Fig. 5. Molecular desorption

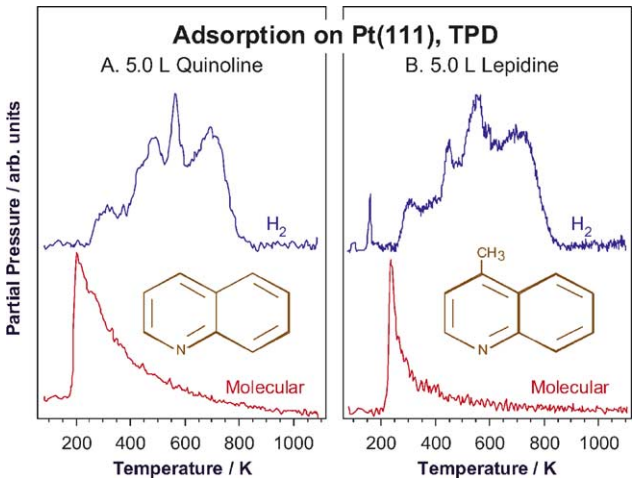

Fig. 5. Hydrogen (2 amu) and molecular (129 and 143 amu, respectively) temperature programmed desorption (TPD) spectra for saturation coverages of quinoline (A, left panel) and lepidine (B, right) on Pt(1 1 1) single crystal surfaces. Molecular desorption starts at 200 and 240 K, respectively, and decomposition and hydrogen evolution is seen in multiple temperature stages starting about 250 K. Significant decomposition of both compounds occurs under vacuum at room temperature, a fact also corroborated by RAIRS.

Table 1
Vibrational assignment of the normal modes detected by RAIRS for quinoline and lepidine adsorbed on Pt(1 1 1) under vacuum and at 100 K

Assignment[a]	Quinoline			Lepidine	
	Liquid [57]	Calculated [53]	On Pt(1 1 1) (this work)	Liquid [56]	On Pt(1 1 1) (this work)
ν_{ip}(CH)	3056, 3036	3377, 3352	3055, 3037		3060, 3036
ν_{ip}(CH)	3005, 2979	3339, 3329	3007, 2949		3006, 2898
ν_{as}(CH_3)					2980, 2952
ν_{s}(CH_3)					2922, 2858
ν_{ip}(ring)	1619, 1593, 1571, 1500	1837, 1812, 1784, 1674	1596, 1571, 1502	1617, 1592, 1573, 1507	1617, 1598, 1572, 1511
ρ_{ip}(CH)	1469	1632	1470	1465	
ρ_{as}(CH_3)					1455, 1421
ρ_{ip}(CH)	1431, 1392	1594, 1537	1432, 1394	1444, 1395	1437, 1394
ρ_{s}(CH_3)					1376
ν_{ip}(ring)	1371, 1031, 1013	1487, 1116, 1073	1373, 1034, 1013	1361, 1027	1365, 1035, 1020
ν_{ip}(ring) + ρ_{ip}(CH)	1314, 1216, 1118, 1095	1455, 1365, 1246, 1198	1315, 1218, 1120, 1098	1294	1308, 1216, 1122, 1085
ρ_{ip}(CH)	1256, 1192, 1140	1387, 1304, 1262	1256, 1197, 1140	1161, 1143	1264, 1246, 1161, 1142
ρ(CH_3)					1065
ω_{oop}(CH)	980, 970, 867, 804	1126, 1094	982, 870, 811	953, 870	982, 940, 869, 814
δ_{ip}(ring)	953	1028	957		958
ω_{oop}(CH) + τ_{oop}(ring)	840			849	843

All wavenumbers are reported in cm^{-1}.
[a] ν, stretching; ρ, rocking; ω, wagging; δ, deformation; τ, twist; ip, in plane; oop, out of plane; as, asymmetric; s, symmetric.

for quinoline and lepidine starts at 200 and 240 K, respectively, and hydrogen production from dehydrogenation of the adsorbed species is detected at temperatures as low as 250 K.

4. Adsorption from liquid solutions

The catalytic hydrogenation of α-ketoesters by platinum modified with chiral cinchona is typically carried out around room temperature. The reactants are also typically dissolved in a liquid solution. This suggests that the solvent may play an important role in the overall performance of these systems. If nothing else, the hydrogen-treated solvents are likely to inhibit the facile dehydrogenation of adsorbed cinchona seen under vacuum. In fact, different solvents do lead to different catalytic behavior. More on this later. In order to characterize the performance of cinchona modifiers in situ under realistic conditions, a setup was developed in our laboratory for the use of infrared spectroscopy to probe liquid–solid interfaces, as indicated in Section 2 (Fig. 2) [50,51].

This instrumentation has proven quite useful for the study of the adsorbed cinchona. Indeed, the infrared spectra obtained for the cinchona–platinum system display a number of intense absorption bands, in particular in the 1100–1700 cm^{-1} range. Several tests were performed to assure that the data correspond to cinchona monolayers, not to dissolved or condensed molecules [50]. First, the spectra obtained using p- and s-polarized light displayed the absorption anisotropy expected from adsorbed species [59,61]. Second, spectra taken using different liquid film thickness did not show the increase in signal expected from dissolved species. Third, the RAIRS spectra obtained for surfaces saturated with cinchonidine from carbon tetrachloride solutions persisted even after flushing the system with fresh pure carbon tetrachloride solvent, an observation that also pointed to the irreversibility of the adsorption. Fourth, no cinchona infrared peaks were detected on oxidized platinum surfaces; only on a surface cleaned by hydrogen pretreatments was it possible to see adsorbed cinchonidine (see later) [62]. Finally, repeated exposures of the surface to fresh cinchona-saturated solutions did not lead to the growth of the infrared absorption bands, as would be the case if they were due to physical condensation (Fig. 6). At this point, we are confident that the spectra we see in our in situ RAIRS studies of the cinchona–platinum system are associated with adsorbed monolayers.

5. Adsorption geometry

Next, a proper assignment of the infrared absorption bands to specific vibrational normal modes of the molecule was needed. For this, a combination of theoretical calculations and comparisons with vibrational spectra from a number of related compounds was performed [63]. Based on that work, the spectra for cinchonidine adsorbed on platinum shown in Fig. 6 was interpreted. In general, in spite of the differences observed between the IR absorption traces for cinchonidine neat versus adsorbed on platinum, it was concluded that the room temperature adsorption of cinchonidine from solution is molecular. Moreover, thanks to the RAIRS surface selection rule mentioned before [59–61], it was also possible to qualitatively estimate the adsorption geometry of the chiral modifier [63]. For starters, the fact that most of the intense bands seen in the 1100–1700 cm^{-1} region of the vibrational

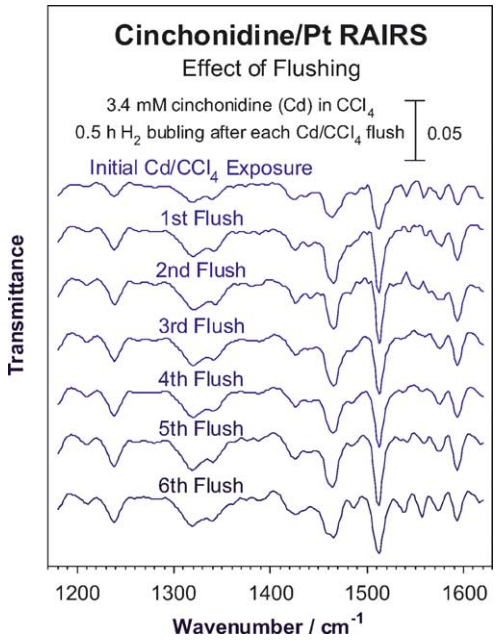

Fig. 6. In situ RAIRS data for cinchonidine adsorbed from 3.4 mM cinchonidine/carbon tetrachloride solutions onto a platinum polycrystalline polished surface. The figure shows the spectra obtained after each of seven consecutive experiments carried out with new fresh solutions. The lack of any significant signal growth after the first exposure rules out the possibility of a build up of condensed layers of pure solid cinchonidine. Additional tests were carried out to also prove that these signals correspond to chemisorbed, not dissolved, species [50]. A detailed vibrational assignment of the RAIRS bands observed was accomplished by using a combination of quantum mechanics computer calculations and comparisons with the spectra of reference compounds [63].

data in Fig. 6 can be ascribed to in-plane deformations of the quinoline ring argues for a tilted geometry of that ring with respect to the surface. Next, the high intensities of the peaks at 1573, 1512, 1422, and 1238 cm^{-1}, which correspond to compression/expansions of the ring along its short axis, compared to the band at 1592 cm^{-1}, which has a dynamic dipole approximately oriented along the N–C2′ bond, suggest an adsorption geometry through the quinoline nitrogen atom and with the adjacent benzene ring away from the surface (for the notation used here, refer to Fig. 1). Lastly, the significant frequency shifts seen in the vibrational modes where the nitrogen atom moves along the short axis of the quinoline ring upon adsorption provide evidence for a degree of sigma bonding between the metal and one of the electron lone pairs of the nitrogen atom. Similar arguments led to the conclusion that the C5-C6-C7-C8 plane of the quinuclidine ring adopts an orientation close to parallel to the surface, and that carbons C7, C8, and C9 interact strongly with the platinum substrate.

An additional complication arises from the fact that the infrared spectra of the adsorbed cinchonidine change dramatically with its concentration in solution. Three regimes were identified for this system [64]: (1) below 5% of saturation of cinchonidine in carbon tetrachloride, where no signals from the adsorbates are visible in the RAIRS data; (2) between 5 and 20%, characterized by spectra with five weak and broad features around 1217, 1255, 1390, 1464, and 1550 cm^{-1}; and (3) above 20% of saturation, which yields data similar to those shown in Fig. 6. As already stated, the high concentration regime corresponds to a tilted adsorption geometry of the quinoline moiety. The intermediate concentrations, on the other hand, are likely to lead to a flat-lying geometry of the aromatic ring instead, with a C8–C9 bond sticking out of the surface [63]. The revealing aspect of these observations in terms of cinchonidine adsorption geometry on platinum surfaces is that they correlate quite nicely with their catalytic activity and enantioselectivity [22,64]. It appears that a flat adsorption is required for the optimal performance of the cinchona/platinum catalytic system, and that is accomplished by using only moderate quantities of the chiral modifier; an excess of cinchona leads to a change in adsorption geometry and a concomitant loss in activity and enantioselectivity.

6. Effect of dissolved gases and solvents

It has already been established that the performance of cinchona chiral modifiers in enantioselective hydrogenation catalysis is affected to a great extent by both the details of the procedures used for catalyst preparation and the reaction conditions. In particular, gases, either in the gas phase or dissolved in the liquid reaction mixture, are known to play an important role in the conditioning and performance of the cinchonidine-modified platinum catalyst used for the hydrogenation of α-ketoesters [37,65–70].

In our in situ RAIRS studies of the adsorption of cinchonidine from carbon tetrachloride solutions onto platinum surfaces [62], it was observed that Ar, N_2, O_2, air, or CO_2 gases none exert any noticeable influence on either the initial uptake or the resulting adlayers once they build up on the surface. On the other hand, H_2 was found to play a unique role, initially facilitating the uptake of cinchonidine but later removing some of the adsorbates from the platinum surface. This is illustrated by the data in Fig. 7, which shows the intensity of the 1512 cm^{-1} RAIRS band of cinchonidine adsorbed on the surface as a function of hydrogen bubbling time. It needs to be remembered that in hydrogenation processes such as those for which the cinchona/Pt system referred to here is used, H_2 is one of the main reactants, and is thereby always present in the solution. Nevertheless, our results indicate that this hydrogen also plays a secondary role in the catalysis. It appears that the H_2 helps reduce the surface and aids in the removal of surface poisons in the early stages of the reaction, but also slowly hydrogenates the aromatic ring of the cinchona, rendering it ineffective for chiral modification.

Our RAIRS investigation of the role of dissolved gases also identified CO as a strong inhibitor which significantly retards the adsorption of cinchonidine [62]. The importance

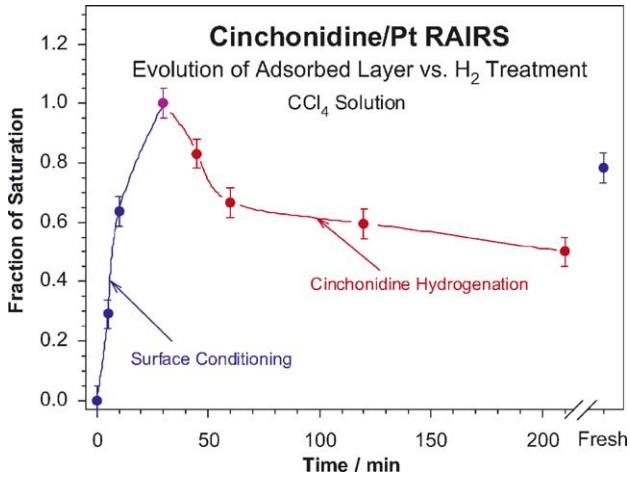

Fig. 7. Effect of bubbling hydrogen on the adsorption of cinchonidine over a platinum surface [62]. The data shown here correspond to the intensity of the RAIRS band at 1512 cm^{-1} as a function of time. Three temporal regimes are clear in this figure: (1) a transient where the Pt surface is gradually cleaned before the maximum in cinchonidine adsorption is reached; (2) the slow disappearance of the adsorbed layer afterwards due to hydrogenation of the adsorbed cinchonidine; and (3) the renewal of the saturated cinchonidine surface after switching to a fresh solution.

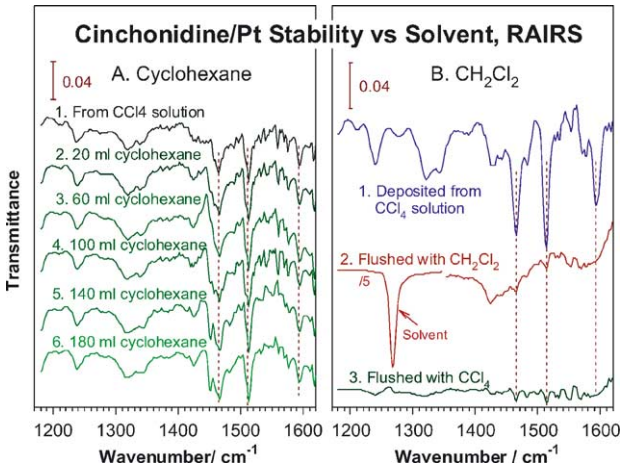

Fig. 8. RAIRS traces from studies on the effect of cyclohexane (A, left panel) and dichloromethane (B, right) solvents on the adsorption of cinchonidine on platinum. In both cases, a clean surface was first exposed to a 3.4 mM cinchonidine carbon tetrachloride solution to build a cinchona surface monolayer (top traces). Those surfaces were then exposed to either cyclohexane or dichloromethane. In the case of cyclohexane (left), a total rinsing with 180 ml in several sequential flushings did not lead to any significant change of the infrared spectra, indicating that the cinchona adsorbed layer is quite stable under these conditions. Similar results were obtained with other non-polar solvents. With dichloromethane, on the other hand, one flush is sufficient to remove most of the adsorbates (right). It is clear that the initial adsorption–desorption equilibria established after exposures of the platinum surface to solutions of cinchonidine in carbon tetrachloride are perturbed by solvents in which the cinchona solubility is much higher.

of this observation to catalysis is illustrated by the reported decrease in ethyl pyruvate hydrogenation rate resulting from addition of formic acid to the reaction mixture, presumably because of surface poisoning by decomposition to CO [71]. It was found in our work that the competitive adsorption of carbon monoxide in the presence of hydrogen, oxygen, and/or cinchonidine displays complex synergies [62]. For instance, adsorbed CO can be removed by H_2 dissolved in the cinchonidine solution (a process that also helps with the adsorption of cinchonidine), but only after a long induction period. On the other hand, the hydrogen-induced CO displacement does not take place at all in the absence of cinchonidine, not even when starting with sub-monolayer coverages of carbon monoxide. Clearly, the adsorption of even a small amount of cinchonidine affects the interaction of CO with the Pt surface. Molecular oxygen can also remove the adsorbed CO (the same as CO can remove adsorbed oxygen), but this does not facilitate cinchonidine adsorption.

The nature of the solvent plays a pivotal role in defining the performance of cinchona-modified platinum catalysts as well. For instance, in the cases of hydrogenation of ethyl pyruvate [19,20] and diones [72], it has been reported that the enantiomeric excess generally decreases with increasing polarity of the solvent. On the other hand, no such correlation could be found in other similar systems [19]. In any case, it has been generally recognized that the effects exerted on these systems by the solvent are related to the solubility of the reactants and modifiers and to the interactions among the solvent, reactants, modifiers and surfaces [20]. More recently, it has also been proposed that solvents influence the conformation of the modifiers, and with that their possible complexation with the reactant [34]. Other effects include the protonation of the quinuclidine nitrogen by acidic solvents [20], and poisoning and/or promotion by species resulting from reactions of the solvent on the surface [73] or the support [74]. Selecting an optimum solvent for a given catalytic process requires a better basic understanding of all these phenomena.

Our studies on the effect of solvents on the adsorption of cinchona have allowed us to identified two broadly different types of behavior exemplified by the data reported for cyclohexane and dichloromethane in Fig. 8 [75]. In these, cinchonidine was first adsorbed from carbon tetrachloride solutions, after which the chemisorbed monolayers were rinsed with a second solvent. In the first case, when using cyclohexane, the adsorbed modifier could not be removed even after repeated flushes with new fresh aliquots of the liquid. This behavior, which indicates a high stability for the chemisorbed cinchona, was qualitatively reproduced with other non-polar solvents, and correlates with a low solubility for cinchonidine in those solvents. With dichloromethane, on the other hand, one flush was sufficient to remove most of the adsorbed molecules; most polar solvents studied led to similar results. It appears that there exist a correlation between solvent polarity and cinchonidine solubility, and that this solubility further regulates the adsorption–desorption equilibrium of cinchonidine on the metal surface. These factors may also play a key role in determining enantioselectivity in chiral-modified catalysts [76,77].

7. Concluding remarks

In the preceding sections we have briefly summarized the results obtained so far by our in situ characterization of the chemisorption of cinchona chiral modifiers from solutions onto platinum surfaces. It has been established that the presence of the hydrogen-treated solvent is critical to inhibit the low-temperature decomposition that is seen under vacuum. It has also been possible to ascribe some of the behavior seen during catalysis directly to the nature of the cinchona chemisorption. For one, the optimal activity and enantioselectivity obtained with intermediate concentrations of the chiral modifier was directly associated to a change in adsorption geometry, from the ideal flat-lying arrangement of the aromatic ring to a tilted mode once the concentration is increased. In addition, the need for hydrogen pretreatment of the platinum catalyst before reaction could be justified by the conditioning needed to facilitate the adsorption of the cinchona on the surface. CO poisoning is explained by competitive adsorption. Finally, the effect of the solvent appears to be at least in part due to changes in the position of the adsorption–desorption equilibrium.

Heterogeneous chiral catalysis has so far had limited use in industrial applications. The main obstacle for the advancement of this field has been the complexity of the systems involved, where even small variations in reaction conditions often lead to large and unpredictable changes in catalytic performance. Our research on the chiral modification of platinum surfaces in situ in the presence of appropriate solutions has indicated that many of the trends seen in catalysis can be tracked down to the properties of the adsorption of the cinchona modifier. The development of a more complete picture of that phenomenon at the molecular level therefore promises to provide the knowledge needed to incorporate chiral modification of heterogeneous catalysts into the commercial synthesis of pharmaceuticals, agrochemicals, and other key compounds.

Acknowledgements

Financial support for this work was provided by the U.S. Department of Energy. Additional funds were provided by the Petroleum Research Fund of the American Chemical Society and by the Merck Research Laboratories.

References

[1] E.L. Eliel, Elements of Stereochemistry, Wiley, New York, 1969.
[2] K. Mislow, Introduction to Stereochemistry, W.A. Benjamin, New York, 1965.
[3] I.-H. Suh, K.H. Park, W.P. Jensen, D.E. Lewis, J. Chem. Educ. 74 (1997) 800.
[4] A.M. Rouchi, Chem. Eng. News 81 (18) (2003) 45.
[5] A. Richards, R. McCague, Chem. Ind. (London) 11 (1997) 422.
[6] S.C. Stinson, Chem. Eng. News 77 (41) (1999) 101.
[7] R. Csuk, B.I. Glänzer, Chem. Rev. 91 (1991) 49.
[8] E. Keinan, K.K. Seth, R. Lamed, J. Am. Chem. Soc. 108 (1986) 3474.
[9] C.W. Bradshaw, W. Hummel, C.-H. Wong, J. Org. Chem. 57 (1992) 1532.
[10] D.P. Martin, D.G. Drueckhammer, J. Am. Chem. Soc. 114 (1992) 7287.
[11] R. Sakowicz, M. Gold, J.B. Jones, J. Am. Chem. Soc. 117 (1995) 2387.
[12] R. Noyori, Asymmetric Catalysis in Organic Synthesis, Wiley, New York, 1994.
[13] R. Schmid, Chimia 50 (1996) 110.
[14] H.U. Blaser, F. Spindler, M. Studer, Appl. Catal. A 221 (2001) 119.
[15] A. Hoek, W.M.H. Sachtler, J. Catal. 58 (1979) 276.
[16] Y. Izumi, Adv. Catal. 32 (1983) 215.
[17] T. Osawa, T. Harada, A. Tai, Catal. Today 37 (1997) 465.
[18] M.A. Keane, Langmuir 13 (1997) 41.
[19] H.-U. Blaser, H.-P. Jalett, M. Müller, M. Studer, Catal. Today 37 (1997) 441.
[20] A. Baiker, J. Mol. Catal. A 115 (1997) 473.
[21] P.B. Wells, A.G. Wilkinson, Top. Catal. 5 (1998) 39.
[22] C. LeBlond, J. Wang, J. Liu, A.T. Andrews, Y.-K. Sun, J. Am. Chem. Soc. 121 (1999) 4920.
[23] T. Mallat, A. Baiker, Appl. Catal. A 200 (2000) 3.
[24] M. Studer, H.U. Blaser, C. Exner, Adv. Synth. Catal. 345 (2003) 45.
[25] H.-U. Blaser, H.P. Jalett, W. Lottenbach, M. Studer, J. Am. Chem. Soc. 122 (2000) 12675.
[26] H.U. Blaser, H.P. Jalett, D.M. Monti, A. Baiker, J.T. Wehrli, Structure-activity and selectivity relationships in heterogeneous catalysis, in: R.K. Grasselli, A.W. Sleight (Eds.), Proceedings of the ACS Symposium on Structure-Activity Relationships in Heterogeneous Catalysis, vol. 67, Boston, MA, 22–27 April 1990, Studies in Surface Science and Catalysis Series, Elsevier, Amsterdam, 1991, pp. 147–155.
[27] A. Pfaltz, T. Heinz, Top. Catal. 4 (1997) 229.
[28] H.U. Blaser, M. Garland, H.P. Jallet, J. Catal. 144 (1993) 569.
[29] R.L. Augustine, S.K. Tanielyan, L.K. Doyle, Tetrahedron: Asymmetry 4 (1993) 1803.
[30] O. Schwalm, B. Minder, J. Weber, A. Baiker, Catal. Lett. 23 (1994) 271.
[31] K.E. Simons, P.A. Meheux, S.P. Griffiths, I.M. Sutherland, P. Johnston, P.B. Wells, A.F. Carley, M.K. Rajumon, M.W. Roberts, A. Ibbotson, Recl. Trav. Chim. Pays-Bas 113 (1994) 465.
[32] J.L. Margitfalvi, M. Hegedüs, J. Catal. 156 (1995) 175.
[33] P.J. Collier, T.J. Hall, J.A. Iggo, P. Johnston, J.A. Slipszenko, P.B. Wells, R. Whyman, Chem. Commun. (1998) 1451.
[34] T. Bürgi, A. Baiker, J. Am. Chem. Soc. 120 (1998) 12920.
[35] H.U. Blaser, D. Imhof, M. Studer, Heterogeneous catalysis and fine chemicals IV, in: H.U. Blaser, A. Baiker, R. Prins (Eds.), Proceedings of the 4th International Symposium on Heterogeneous Catalysis and Fine Chemicals, vol. 108, 8–12 September 1996, Basel, Switzerland, Studies in Surface Science and Catalysis Series, Elsevier, Amsterdam, 1997, pp. 175–182.
[36] J.T. Wehrli, A. Baiker, D.M. Monti, H.U. Blaser, J. Mol. Catal. 49 (1989) 195.
[37] T. Mallat, S. Frauchiger, P.J. Kooyman, M. Schürch, A. Baiker, Catal. Lett. 63 (1999) 121.
[38] T.J. Hall, J.E. Halder, G.J. Hutchings, R.L. Jenkins, P. Johnston, P. McMorn, P.B. Wells, R.P.K. Wells, Top. Catal. 11/12 (2000) 351.
[39] U. Böhmer, F. Franke, K. Morgenschweis, T. Bieber, W. Reschetilowski, Catal. Today 60 (2000) 167.
[40] P.A. Meheux, A. Ibbotson, P.B. Wells, J. Catal. 128 (1991) 387.
[41] Y. Sun, R.N. Landau, J. Wang, C. LeBlond, D.G. Blackmond, J. Am. Chem. Soc. 118 (1996) 1348.
[42] J. Wang, C. Leblond, C.F. Orella, Y. Sun, J.S. Bradley, D.G. Blackmond, Heterogeneous catalysis and fine chemicals IV, in: H.U. Blaser, A. Baiker, R. Prins (Eds.), Proceedings of the 4th International Sym-

posium on Heterogeneous Catalysis and Fine Chemicals, vol. 108, 8–12 September 1996, Basel, Switzerland, Studies in Surface Science and Catalysis Series, Elsevier, Amsterdam, 1997, pp. 183–190.
[43] D. Ferri, T. Bürgi, A. Baiker, Chem. Commun. (2001) 1172.
[44] D. Ferri, T. Bürgi, J. Am. Chem. Soc. 123 (2001) 12074.
[45] W. Chu, R.J. LeBlanc, C.T. Williams, Catal. Commun. 3 (2002) 547.
[46] H. Hoffmann, P.R. Griffiths, F. Zaera, Surf. Sci. 262 (1992) 141.
[47] D. Chrysostomou, F. Zaera, J. Phys. Chem. B 105 (2001) 1003.
[48] T.V.W. Janssens, F. Zaera, J. Catal. 208 (2002) 345.
[49] V.P. Zhdanov, B. Kasemo, Surf. Sci. 415 (1998) 403.
[50] J. Kubota, Z. Ma, F. Zaera, Langmuir 19 (2003) 3371.
[51] F. Zaera, Int. Rev. Phys. Chem. 21 (2002) 433.
[52] J.M. Bonello, R.M. Lambert, Surf. Sci. 498 (2002) 212.
[53] I. Bandyopadhyay, S. Manogaran, Indian J. Chem. A 39 (2000) 189.
[54] A.E. Özel, Y. Büyükmurat, S. Akyüz, J. Mol. Struct. 565/566 (2001) 455.
[55] P. Chiorboli, A. Bertoluzza, Ann. Chim. 49 (1959) 245.
[56] A.R. Katritzky, R.A. Jones, J. Chem. Soc. (1960) 2942.
[57] S.C. Wait Jr., J.C. McNerney, J. Mol. Spectrosc. 34 (1970) 56.
[58] G. Socrates, Infrared Characteristic Group Frequencies: Tables and Charts, second ed., Wiley, Chichester, 1994.
[59] R.G. Greenler, J. Chem. Phys. 44 (1966) 310.
[60] F. Zaera, H. Hoffmann, P.R. Griffiths, J. Electron. Spectrosc. Relat. Phenom. 54/55 (1990) 705.
[61] F. Zaera, in: J.H. Moore, N.D. Spencer (Eds.), Encyclopedia of Chemical Physics and Physical Chemistry, vol. 2, IOP Publishing Inc., Philadelphia, 2001, pp. 1563–1581.
[62] Z. Ma, J. Kubota, F. Zaera, J. Catal. 219 (2003) 404.
[63] W. Chu, R.J. LeBlanc, C.T. Williams, J. Kubota, F. Zaera, J. Phys. Chem. B 107 (2003) 14365.
[64] J. Kubota, F. Zaera, J. Am. Chem. Soc. 123 (2001) 11115.
[65] H.U. Blaser, H.P. Jalett, D.M. Monti, J.T. Wehrli, Appl. Catal. 52 (1989) 19.
[66] I.M. Sutherland, A. Ibbotson, R.B. Moyes, P.B. Wells, J. Catal. 125 (1990) 77.
[67] R.L. Augustine, S.K. Tanielyan, J. Mol. Catal. A 118 (1997) 79.
[68] C. LeBlond, J. Wang, A.T. Andrews, Y.-K. Sun, Top. Catal. 13 (2000) 169.
[69] V. Morawsky, U. Prüße, L. Witte, K.-D. Vorlop, Catal. Commun. 1 (2000) 15.
[70] M. Bartók, G. Szöllösi, K. Balázsik, T. Bartók, J. Mol. Catal. A 177 (2002) 299.
[71] H.U. Blaser, H.P. Jalett, J. Wiehl, J. Mol. Catal. 68 (1991) 215.
[72] R.P.K. Wells, N.R. McGuire, X.B. Li, R.L. Jenkins, P.J. Collier, R. Whyman, G.J. Hutchings, Phys. Chem. Chem. Phys. 4 (2002) 2839.
[73] M. von Arx, T. Mallat, A. Baiker, Top. Catal. 19 (2002) 75.
[74] M. Bartók, K. Balázsik, G. Szöllösi, T. Bartók, J. Catal. 205 (2002) 168.
[75] Z. Ma, J. Kubota, F. Zaera, J. Am. Chem. Soc., submitted.
[76] A. Gamez, J. Köhler, J. Bradley, Catal. Lett. 55 (1998) 73.
[77] Y. Nitta, Top. Catal. 13 (2000) 179.